Published OnlineFirst October 12, 2012; DOI: 10.1158/0008-5472.CAN-12-0088

NF-κB Activity Regulates Mesenchymal Stem Cell Accumulation at Tumor Sites

Ryosuke Uchibori[1], Tomonori Tsukahara[1], Hiroyuki Mizuguchi[4], Yasushi Saga[2], Masashi Urabe[1], Hiroaki Mizukami[1], Akihiro Kume[1], and Keiya Ozawa[1,3]

Abstract

Mesenchymal stem cells (MSC) accumulate at tumor sites when injected into tumor-bearing mice, perhaps offering cellular vectors for cancer-targeted gene therapy. However, the molecular mechanisms involved in MSC targeting the tumors are presently little understood. We focused on MSC–endothelial cell (EC) adhesion following TNF-α stimulation in an attempt to elucidate these mechanisms. Interestingly, stimulation of MSCs with TNF-α enhanced the adhesion of MSCs to endothelial cells *in vitro*. This adhesion was partially inhibited by blocking antibodies against vascular cell adhesion molecule-1 (VCAM-1) and very late antigen-4 (VLA-4). It is well known that TNF-α induces VCAM-1 expression via the NF-κB signaling pathway. Parthenolide has an anti-inflammatory activity and suppressed NF-κB activity by inhibition of IκBα phosphorylation after TNF-α stimulation and strongly inhibited TNF-α–induced VCAM-1 expression on MSCs. *In vivo* imaging using luciferase-expressing MSCs revealed that the bioluminescent signal gradually increased at tumor sites in mice injected with untreated MSCs. In contrast, we observed very weak signals at tumor sites in mice injected with parthenolide-treated MSCs. Our results suggest that NF-κB activity regulates MSC accumulation at tumors, by inducing VCAM-1 and thereby its interaction with tumor vessel endothelial cells. These findings have implications for the ongoing development of efficient MSC-based gene therapies for cancer treatment. *Cancer Res; 73(1); 1–9. ©2012 AACR.*

Introduction

Mesenchymal stem cells (MSC) are nonhematopoietic stem cells with high-proliferative potency and have the ability to differentiate into multiple lineages. They are detected in several adult and fetal tissues, including bone marrow, adipose tissue, and umbilical cord blood. MSCs have generated a great deal of interest in their potential use in regenerative medicine due to their ability to migrate to damaged tissues and to produce cytokines. Furthermore, MSCs can be easily genetically modified with viral vectors to be used as novel cellular vehicles in gene therapy protocols. MSCs are also used to treat severe acute GVHD, because they accumulate at inflammatory lesions and have immunomodulatory activity.

Interestingly, recent studies indicated that MSCs also have the ability to accumulate in tumors. Therefore, they can be used as cellular vehicles for cancer-targeted gene therapy. Intravenous injection of engineered MSCs expressing IFN-β was reported to inhibit the growth of melanoma pulmonary metastasis (1) and breast cancer (2) in mice and also prolonged the survival of mice with glioma xenografts (3). Furthermore, interleukin (IL)-12, which improves immune surveillance against cancer cells (4), and chemokine CX3CL1 (fractalkine), which is able to activate T cells and natural killer (NK) cells (5), were used as therapeutic molecules. We have also shown that retrovirus vector–producing MSCs also effectively inhibit tumor growth (6). In this context, treatment has been developed using retroviral vectors expressing the thymidine kinase of herpes simplex virus combined with the prodrug ganciclovir.

The ability of MSCs to specifically localize the multiple tumors, makes them extremely attractive for targeted cancer therapy. The most likely cause of preferential migration was considered to be the release of chemotactic gradients from tumor tissues. MSCs have a variety of chemokine and cytokine receptors and respond functionally to ligands *in vitro*. Tumors are known to produce a large amount of chemokines and cytokines, which could serve as ligands for the receptors on MSCs (7). Therefore, the mechanism of MSC accumulation at the site of tumors seems to be based on their migratory ability. Nevertheless, although various growth factors and chemokines, such as platelet-derived growth factor (PDGF), hepatocyte growth factor (HGF), and stromal cell–derived factor-1α (SDF-1α) may be involved, the detailed molecular mechanisms of MSC accumulation at tumors are poorly understood.

Authors' Affiliations: [1]Division of Genetic Therapeutics, Center for Molecular Medicine; [2]Department of Obstetrics and Gynecology; [3]Division of Hematology, Department of Medicine, Jichi Medical University, Tochigi; and [4]Department of Biochemistry and Molecular Biology, Osaka University, Osaka, Japan

Note: Supplementary data for this article are available at Cancer Research Online (http://cancerres.aacrjournals.org/).

Corresponding Author: Keiya Ozawa, Division of Genetic Therapeutics, Center for Molecular Medicine, Jichi Medical University, 3311-1 Yakushiji, Shimotsuke, Tochigi 329-0498, Japan. Phone: 81-285-58-7402; Fax: 81-285-44-8675; E-mail: kozawa@jichi.ac.jp

doi: 10.1158/0008-5472.CAN-12-0088

Published OnlineFirst October 12, 2012; DOI: 10.1158/0008-5472.CAN-12-0088

In the present study, we focused on MSC–endothelial cell (EC) adhesion following TNF-α stimulation in an attempt to elucidate the mechanism of MSC accumulation at tumors.

Materials and Methods

Cell culture

Bone marrow–derived human MSCs (Lonza Walkersville, Inc.) were cultured in mesenPRO RS medium (Invitrogen). HEK293-derived AD-293 cells (Stratagene), human embryonic fibroblasts WI-38 (RIKEN BRC), human colon adenocarcinoma cell lines SW480 (Cell Resource Center for Biomedical Research Institute of Development, Aging and Cancer, Tohoku University, Miyagi, Japan), and SW480/RFP that was generated by transduction of SW480 with red fluorescent protein-expressing retrovirus vectors (RV-RFP), were grown in Dulbecco's Modified Eagle's Medium (DMEM)/F-12 medium (Invitrogen) supplemented with 10% FBS, 100 U/mL penicillin, and 100 μg/mL streptomycin (P/S). Human endothelial progenitor cells (ApproCell Inc.) were cultured in endothelial progenitor cells grown medium (ApproCell Inc.). Human colon adenocarcinoma cell lines Colo205 (Cell Resource Center for Biomedical Research Institute of Development, Aging and Cancer Tohoku University) and Colo205/RFP that was generated by transduction with RV-RFP, were grown in RPMI medium (Invitrogen) supplemented with FBS and P/S. All cultures were kept in an incubator at 37°C and 5% CO_2.

Adenoviral vectors

Adenoviral vectors expressing a GFP were constructed by an improved *in vitro* ligation method (8, 9). The shuttle plasmid pHMCA5-GFP contains a CA promoter (a β-actin promoter/CMV enhancer with a β-actin intron), *GFP* gene, and a bovine growth hormone (BGH) polyadenylation signal, all of which are flanked by I-CeuI and PI-SceI restriction sites. I-CeuI/PI-SceI–digested pHMCA5-GFP was ligated with I-CeuI/PI-SceI–digested pAdHM4, resulting in pAdHM4-CAGFP. pAdHM41-K7-CAGFP was constructed by ligation of I-CeuI/PISceI–digested pHMCA5-GFP with I-CeuI/PI-SceI–digested pAdHM41-K7 (10). Viruses (Ad5-GFP and AdK7-GFP) were generated by transfection of PacI-digested pAdHM4-CAGFP and pAdHM41-K7-CAGFP, respectively, into AD-293 cells with SuperFect (Qiagen) according to the manufacturer's instructions. Each virus was purified by $CsCl_2$ step gradient ultracentrifugation followed by $CsCl_2$ linear gradient ultracentrifugation. Virus particles and biologic titers of each vector preparation were determined as described by Mittereder and colleagues (11). We also created Ad vectors expressing luciferase (Luc) using the shuttle plasmid pHMCA5-Luc, which contains the *Luc* gene derived from pELuc-test (Toyobo Co. Ltd.). MSCs and fibroblasts were seeded in culture plates or flasks at a density of 1×10^4 cells/cm^2, and the next day the cells were treated with each adenovirus vector for 1.5 hours. The medium containing the vectors was removed and replaced with fresh medium.

Animal models

All animal experiments were approved by the Jichi Medical University (Tochigi, Japan) ethics committee and carried out in accordance with the NIH Guide for the Care and Use of Laboratory Animals. To create tumor-bearing mice, SW480/RFP cells (3×10^6) were subcutaneously inoculated into 4- to 6-week-old male Balb/c nu/nu mice (Clea Japan Inc.). The mice were used for experiments 7 days after inoculation.

Immunohistchemistry

Cultured MSCs and fibroblasts were transduced with AdK7-GFP at a concentration of 3,000 virus particles per cell (vp/cell). Two days after transduction, cells were injected into the left ventricular cavities (1×10^6, day 0) of tumor-bearing mice. Mice were sacrificed on day 4, and 7-μm serial cryosections from frozen tissues were processed. Immunohistochemistry was conducted with fluorescein isothiocyanate (FITC)-conjugated anti-GFP antibody (ab6662; Abcam Inc.) on tumor cryosections to detect MSCs or fibroblasts. Nuclei were stained with 4′,6-diamidino-2-phenylindole (DAPI; Vector Laboratories, Inc.). Images were obtained with a fluorescence microscope (BZ-9000; Keyence). SW480/RFP cells (3×10^6) were subcutaneously inoculated into 4- to 6-week-old male Balb/c nu/nu mice. Mice were sacrificed on day 11, serial sections from tumor tissues were processed. Immunohistochemistry was conducted with anti-mouse CD34 monoclonal antibody (MEC14.7; GeneTex Inc.) on tumor section to detect tumor blood vessels. Histofine Simple Stain Mouse MAX PO (Nichirei Biosciences, Inc.) was used as a horseradish peroxidase–conjugated secondary antibody, and 3,3′-diaminobenzidine (DAB) solution was used for brown color development. Sections were then counterstained with Hematoxylin (Wako Pure Chemical Industries, Ltd.). Images were obtained with a fluorescence microscope (BZ-9000).

In vivo imaging of homing ability to tumors

Cultured MSCs and fibroblasts were transduced with AdK7-Luc at a concentration of 3,000 and 680 vp/cell, respectively. Two days after transduction, cells were injected into the left ventricular cavities (1×10^6, day 0) of tumor-bearing mice, and then optical bioluminescence imaging was conducted to periodically trace the cells using an *in vivo* imaging system (IVIS; Xenogen). To detect bioluminescence from MSCs or fibroblasts, the reporter substrate D-luciferin (Ieda Chemical Co., Ltd.) was injected into the mouse peritoneum (75 mg/kg body weight) for scanning. The luminescent intensity at tumor sites was analyzed using Living Image software (Xenogen).

In vitro migration assays

Cultured MSCs or fibroblasts were serum-starved for 12 hours. One hundred microliters of tumor conditioning medium (CM), or serum-free medium supplemented with PDGF-BB (10 ng/mL), HGF (30 ng/mL), fibroblast growth factor-β (FGF-β; 20 ng/mL), SDF-1α (150 ng/mL), VEGF-A (25 ng/mL), or monocyte chemoattractant protein-1 (MCP-1; 100 ng/mL) was added to the lower wells of migration chambers (8-μm pore size; Neuro Probe, Inc.); MSCs or fibroblasts (4×10^4) were added to the upper wells. All recombinant proteins were purchased from R&D systems Inc.. Medium alone (DMEM/F-12) was used as a negative control and treatment with 30% FBS was the positive control. After incubation for 24 hours at

Published OnlineFirst October 12, 2012; DOI: 10.1158/0008-5472.CAN-12-0088

37°C, cells were labeled with CyQUANT NF dye, and cells attached to the lower surface of the filters were detached with trypsin. Fluorescent intensity was measured using a fluoroscan, and the number of adherent cells was quantified using a standard curve constructed by a known number of cells.

Flow cytometric analysis of adhesion molecules

Cultured MSCs, fibroblasts or endothelial cells were stimulated with TNF-α and harvested by trypsinization. Cell aliquots were incubated with FITC-conjugated monoclonal antibodies (BD) against vascular cell adhesion molecule-1 (VCAM-1), CD49d, CD29 (Integrin-β1), and analyzed by flow cytometry (FACScan; BD Biosciences). For each analysis, an aliquot of cells was also stained with isotype control immunoglobulin G (IgG)–conjugated to FITC as a negative control.

Assay for TNF-α produced in tumor-bearing mice

SW480/RFP (3×10^6) cells were subcutaneously inoculated into nude mice. Seven days after inoculation, mice were anesthetized with an overdose of isoflurane inhalation. The blood was collected and allowed to coagulate overnight on ice. After centrifugation of the samples (2,000 × *g*, 30 minutes, 4°C), the serum was removed and stored at −70°C. Tumor, spleen, and liver tissues were homogenized in 1.5 mL of α-minimum essential medium using a tissue homogenizer. The homogenates were then centrifuged (2,000 × *g*, 30 minutes, 4°C), and the supernatant was removed and recentrifuged (14,000 × *g*, 30 minutes, 4°C). Serum and supernatants from tissue homogenates were kept at −70°C until use. TNF-α was assayed using a commercially available ELISA kit (mouse TNF-α Instant ELISA; Bender MedSystems) according to the manufacturer's protocols.

In vitro adhesion assays

For adhesion assays, endothelial cells (at 4 passages) were cultured to confluence on fibronectin-coated 96-well plates (20 ng/mL; Sigma-Aldrich, Inc.) and treated with TNF-α (10 ng/mL) for 12 hours before assaying. MSCs and fibroblasts were treated with TNF-α (10 ng/mL) 12 hours before the adhesion assays and incubated with isotype control IgG or anti-VCAM-1 or very late antigen-4 (VLA-4; 10 μg/mL) monoclonal antibodies (mAb) for 1 hour. Cells were labeled with CyQUANT NF dye, and 1×10^4 cells were seeded onto endothelial cells. After 30 minutes of incubation at 37°C, wells were washed thoroughly 3 times with PBS to remove nonadherent cells. Fluorescent intensity was measured using a fluoroscan, and the number of adherent cells was quantified using a standard curve constructed by a known number of cells. In some experiments, MSCs and fibroblasts were pretreated for adhesion studies with one of the following substances: TNF-α (10 ng/mL), anti-VCAM-1 antibody (mouse monoclonal anti-rat, clone 5F10, 10 μg/mL, Eurogentec), or anti-VLA-4 antibody (mouse monoclonal anti-rat, clone 1A29, 10 μg/mL, Research Diagnostics).

Parthenolide treatment of MSCs

Parthenolide (Biomol) was reconstituted in dimethyl sulfoxide (DMSO; Sigma-Aldrich, Inc.) to a stock concentration of 0.4 mol/L and subsequently diluted in PBS. MSCs were treated with parthenolide (5 μmol/L) for 6 hours before experiments. To assess the effect of parthenolide treatment of transgene expression, cells were reseeded into 96-well plates, and luciferase assays were conducted using luciferase-expressing MSCs. Cell viability after parthenolide treatment was also examined with Cell Proliferation Kit II [2,3-bis[2-methoxy-4-nitro-S-sulfophenynl]H-tetrazolium-5 carboxanilide inner salt (XTT); Roche Diagnostics GmbH] according to the manufacturer's instructions.

Western blotting

Western blot analysis was conducted to measure the NF-κB pathways. Next, MSCs were pretreated with parthenolide or vehicle (DMSO) for 6 hours, and then cultured with TNF-α (10 ng/mL) for 3 minutes. Cells were lysed in radioimmunoprecipitation assay (RIPA) buffer containing protease inhibitor (Pierce Biotechnology). Protein extracts were electrophoresed on a 4% to 12% Bis–Tris gel (Invitrogen), and transferred to polyvinylidene difluoride (PVDF) membranes. Membranes were incubated in PVDF blocking reagent (TOYOBO), and then incubated with primary antibodies against the following proteins: IκBα, phospho-IκBα (Ser32), NF-κB p65, phospho-NF-κB p65 (Ser536), and α-tublin (Cell Signaling Technology), followed by incubation with horseradish peroxidase-conjugated goat anti-rabbit IgG or -mouse IgG1 secondary antibody, and detected using a Western blotting detection system (GE Healthcare).

Immunocytochemistory

To visualize p65 nuclear translocation, MSCs were pretreated with parthenolide or vehicle (DMSO) for 6 hours and then cultured with TNF-α (10 ng/mL) for 20 minutes. Cells were fixed with 4% fomaline and permiabilized with Triron-X 100. After washing with PBS, slides were incubated with rabbit anti-p65 antibody (Cell Signaling Technology), followed by incubation with Alexa Fluor 488–conjugated goat anti-rabbit IgG secondary antibody. The actin cytoskeleton was stained with Alexa Fluor 546–conjugated phalloidin (Invitrogen); nuclei were stained with 1,5-bis{[2-(di-methylamino) ethyl]amino}-4,8-dihydroxyanthracene-9,10-dione (DRAQ)-5 dye (Invitrogen). Cells were examined using Keyence BZ-9000.

Results

In vivo imaging of MSC accumulation in tumors

We used bone marrow–derived human MSCs, which expressed characteristic phenotypic markers for MSCs and differentiated into adipocyte, osteocyte, and chondrocyte under specific culture conditions (Supplementary Fig. S1). Then, fiber-modified adenovirus vectors (AdK7) were used for efficient transduction of MSCs and fibroblasts in this study. When the cells were transduced with GFP-expressing AdK7 vectors at a density of 3,000 vp/cell, transduction efficiency was almost 100% (Supplementary Fig. S2A and S2B). The bioluminescent intensity of MSCs transduced with luciferase-expressing Ad vectors at 3,000 vp/cell was equal to that of fibroblasts transduced at 680 vp/cell (Supplementary Fig. S2C). Mice injected with GFP-expressing MSCs or fibroblasts were sacrificed 4 days after injection for immunohistochemical analysis.

Published OnlineFirst October 12, 2012; DOI: 10.1158/0008-5472.CAN-12-0088

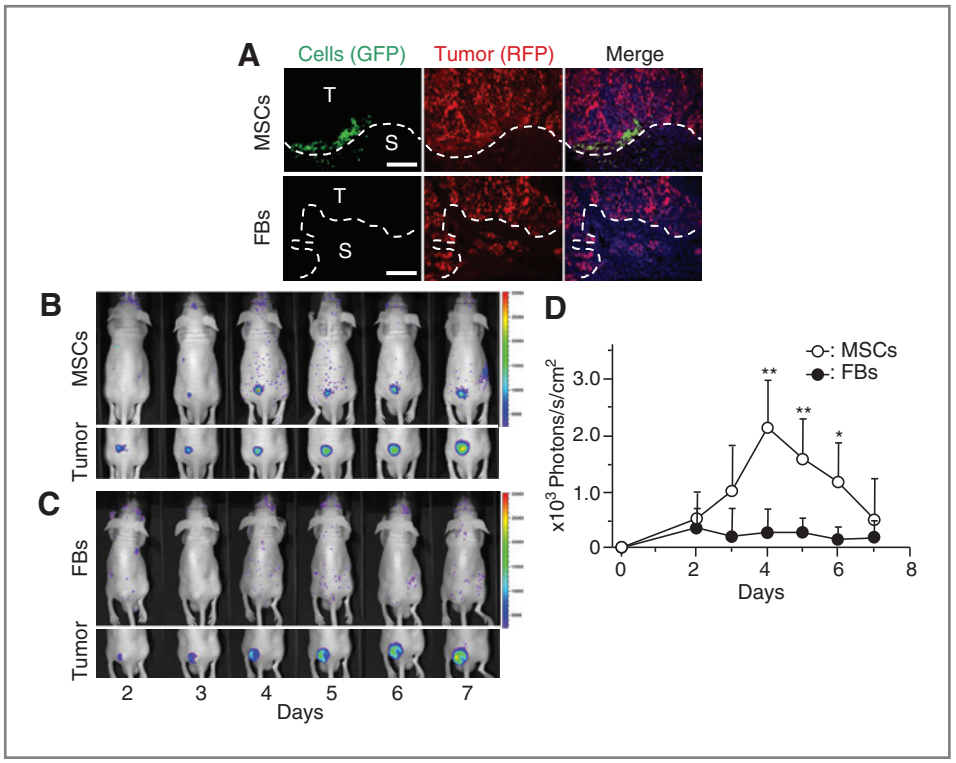

Figure 1. Tumor homing ability of MSCs *in vivo*. A, subcutaneous tumors were induced by injection of SW480/RFP cells (3×10^6) in nude mice (day 0). Cultured MSCs or fibroblasts were transduced with GFP-expressing adenovirus vectors 2 days before injection (day 5) and were injected into the left ventricular cavity (1×10^6, day 7). Mice were sacrificed on day 11, and immunohistochemistry was conducted with anti-GFP antibody on tumor cryosections to detect MSCs or fibroblasts. Top, fluorescent microscopy view of MSC detection; MSCs (left), RFP-labeled tumor cells (center), nucleic staining with DAPI and merge (right). Bottom, fluorescent microscopy view of fibroblast detection; fibroblasts (left), RFP-labeled tumor cells (center), nucleic staining with DAPI and merge (right). Data shown are from 1 representative experiment of 3 carried out. Scale bar, 100 μm. S, stroma; T, tumor. B, luciferase-expressing MSCs were injected into tumor-bearing mice via the left ventricular cavity (1×10^6, day 7). Optical bioluminescence imaging was conducted to periodically trace the cells using IVIS. Top, biodistribution of MSCs as detected by luminescence. Bottom, tumor site detected by red fluorescence. Data shown are from 1 representative experiment of 8 carried out. C, luciferase-expressing fibroblasts were injected into tumor-bearing mice and IVIS imaging was conducted as described earlier. Top, biodistribution of fibroblasts indicated by luminescence. Bottom, tumor site indicated by red fluorescence. Data shown are from 1 representative experiment of 7 carried out. D, bioluminescent intensity at tumor sites was quantified using analysis software. The data are expressed as mean ± SD ($n = 8$ for MSCs and $n = 7$ for fibroblasts). *, $P < 0.05$; **, $P < 0.01$ compared with fibroblasts at the same time.

MSCs identified with anti-GFP antibody were detected in the boundaries of tumors and tumor stroma. However, we found no GFP-positive fibroblasts in the tumor tissues (Fig. 1A). We also used bioluminescence imaging to quantitatively investigate the tumor tropism of MSCs. We injected luciferase-expressing MSCs or fibroblasts into mice through the left ventricular cavity, and then conducted optical bioluminescence imaging to periodically trace the cells using IVIS. In mice injected with luciferase-expressing MSCs, optical bioluminescence at tumor sites became pronounced over time (Fig. 1B), and signal intensity gradually increased (Fig. 1D). In contrast, we observed no signal at the tumor sites in mice injected with luciferase-expressing fibroblasts (Fig. 1C and D).

In vitro migration assays

We analyzed the effects of several growth factors (specifically PDGF-BB, HGF, and VEGF), chemokines (specifically MCP-1 and SDF-1α), and SW480 culture–conditioned medium on MSC and fibroblast migration. These factors are commonly expressed in tumor tissues, and are thought to be potential mediators of MSC tropism. We also used serum-free medium as a negative control and medium containing 30% FBS as a positive control. Migration was quantified by direct labeling and counting of cells by a fluorometer (Fluoroskan Ascent FL; Thermo Labsystems). Exposure to PDGF, HGF, or conditioned medium from SW480 cells stimulated significant MSC migration, whereas VEGF and SDF-1α had no significant effect as compared with serum-free medium (Fig. 2). We compared the migration capacity of MSCs and fibroblasts, the factors that attracted MSCs also induced migration of fibroblasts. Rather, it seems that fibroblasts were more strongly attracted to these factors than MSCs.

In vitro adhesion assays

The tumors generated in mice in this study strongly induced tumor stroma with defined blood vessels, and MSCs specifically accumulated in this stroma (Fig. 3A). Therefore, we propose a hypothesis as follows: factors, as indicated in Fig. 2, attract both MSCs and fibroblasts to the tumor microenvironment, but importantly, MSCs significantly adhere to endothelial cells as

Published OnlineFirst October 12, 2012; DOI: 10.1158/0008-5472.CAN-12-0088

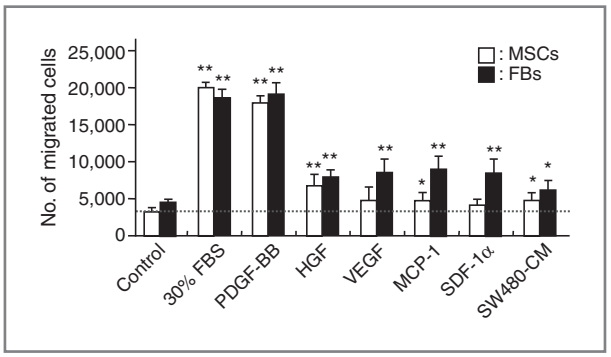

Figure 2. Migratory capacity of MSCs and fibroblasts (FB) in response to growth factors, chemokines, and conditioned medium from SW480 cells. MSCs or fibroblasts were serum-starved for 12 hours. Cells (4×10^4) were added to upper wells of migration chambers. Then, tumor conditioning medium, serum-free medium supplemented with PDGF-BB (10 ng/mL), HGF (30 ng/mL), SDF-1α (150 ng/mL), VEGF-A (25 ng/mL), or MCP-1 (100 ng/mL) were added to the lower wells. Treatment with medium alone (DMEM/F-12) was used as a negative control and treatment with 30% FBS was used as the positive control. The contents of the upper wells and lower wells were separated by polycarbonate filters (8 μm). The data are expressed as mean ± SD ($n = 8$ per cell type). Values are presented as mean ± SE. *, $P < 0.05$ and **, $P < 0.01$ compared with each control.

compared with fibroblasts. Therefore, only MSCs migrate and accumulate at tumor sites via blood vessels in tumor stroma. We speculated that inflammatory cytokines (specifically TNF-α) are required for induction of adhesion molecule expression. First, we measured TNF-α levels in tumor tissues by ELISA. The TNF-α level is significantly higher in tumor tissues as compared with liver and spleen (Fig. 3B). Similar results were also observed in another experiments using Colo205 tumor cells (Supplementary Fig. S3). Then, we assessed the expression of adhesion molecules on endothelial cells, MSCs, and fibroblasts by fluorescence-activated cell sorting analysis. After TNF-α stimulation, endothelial cells and MSCs significantly expressed adhesion molecules including VCAM-1 and VLA-4, compared with fibroblasts (Fig. 3C). We also examined the *in vitro* adhesion of MSCs to endothelial cells. MSCs effectively adhered to endothelial cells as compared with fibroblasts (Fig. 3D). Furthermore, this adhesion was partially inhibited by blocking antibodies against VCAM-1 and VLA-4.

Effects of parthenolide on MSC migration and adhesion

We propose a hypothesis that if TNF-α–induced VCAM-1 expression is inhibited, MSC accumulation at tumors is also attenuated. It is well known that TNF-α induces VCAM-1 expression through the NF-κB signaling pathway. We used parthenolide, a sesquiterpene lactone that occurs naturally in the Feverfew plant. Although parthenolide has several biologic activities, we focused on its suppressive effect on NF-κB activity. At first, there were no differences in migratory capacity toward growth factors or chemokines with or without parthenolide treatment (Fig. 4A). Next, we assessed the inhibitory effect of parthenolide on NF-κB activity: MSCs were pretreated for 6 hours, and then were stimulated with TNF-α for 3 minutes. Parthenolide suppressed p65 nuclear translocation through the inhibition of IκBα phosphorylation (Fig. 4B and C) and strongly inhibited the TNF-α–induced VCAM-1 expression on MSCs (Fig. 4D). Consequently, and MSC–EC adhesion was strongly inhibited by parthenolide treatment similarly to anti-VCAM-1 blocking antibody (Fig. 4E).

In vivo imaging of parthenolide-treated MSCs

First, we examined the effect of parthenolide treatment on transgene expression and cell viability. There were no significant effects on transgene expression and cell viability after parthenolide treatment (Fig. 5A and B). Next, we conducted *in vivo* imaging using IVIS. We observed definite bioluminescence at tumor sites in the mice injected with untreated MSCs (Fig. 5C), and bioluminescent intensity was gradually increased (Fig. 5E), as indicated earlier (Fig. 1B). In contrast, we could not observe definite accumulation at the tumor sites in mice injected with parthenolide-treated MSCs (Fig. 5D and E). Similar results were also obtained by experiments using Colo205 tumor-bearing mice (Supplementary Fig. S4).

Discussion

In this study, we showed that MSC accumulation at tumor sites would be related not only to migratory capacity toward growth factors and chemokines, but also to MSC–EC adhesion following activation by TNF-α. We further showed that NF-κB activity regulates MSC accumulation at tumor sites through the induction of VCAM-1 expression and the resultant interaction with tumor blood vessel endothelial cells.

It is thought that MSCs are mobilized into action following tissue damage, such as injury or inflammation typically accompanied by the release of inflammatory cytokines from the damaged tissues, leading to the recruitment of MSCs to the target. Tumors have a microenvironment consisting of large numbers of inflammatory cells (12). This microenvironment promotes the recruitment of MSCs via various soluble factors secreted by the tumor and inflammatory cells, including EGF, VEGF-A, FGF, PDGF, SDF-1α, IL-8, IL-6, granulocyte colony-stimulating factor (G-CSF), granulocyte-macrophage colony-stimulating factor (GM-CSF), MCP-1, HGF, TGF-β1, and urokinase-type plasminogen activator (uPA; ref. 13). However, in our experimental settings, although systemically injected MSCs accumulated at the tumors, subcutaneously injected MSCs did not (data not shown). We also compared the migration capacity of MSCs and fibroblasts toward growth factors and chemokines *in vitro*. Rather, it seems that fibroblasts were more strongly attracted to these factors than MSCs. Our results suggest that the mechanism of MSC accumulation cannot be explained solely by cytokine-mediated migration. Therefore, we need different viewpoints to clarify the mechanism.

The tumors generated in this study strongly induced tumor stroma with large numbers of blood vessels, and MSCs in particular accumulated in the boundaries between the tumors and tumor stroma. Furthermore, MSC accumulation at the site of the tumors was observed only when cells were injected via the left ventricular cavity. Therefore, we focused on MSC–EC adhesion to elucidate the mechanisms involved.

It has previously been reported that the interaction of MSCs with the vascular endothelium resembles leukocyte chemotaxis (14). To analyze these interactions, we referred to a model

Published OnlineFirst October 12, 2012; DOI: 10.1158/0008-5472.CAN-12-0088

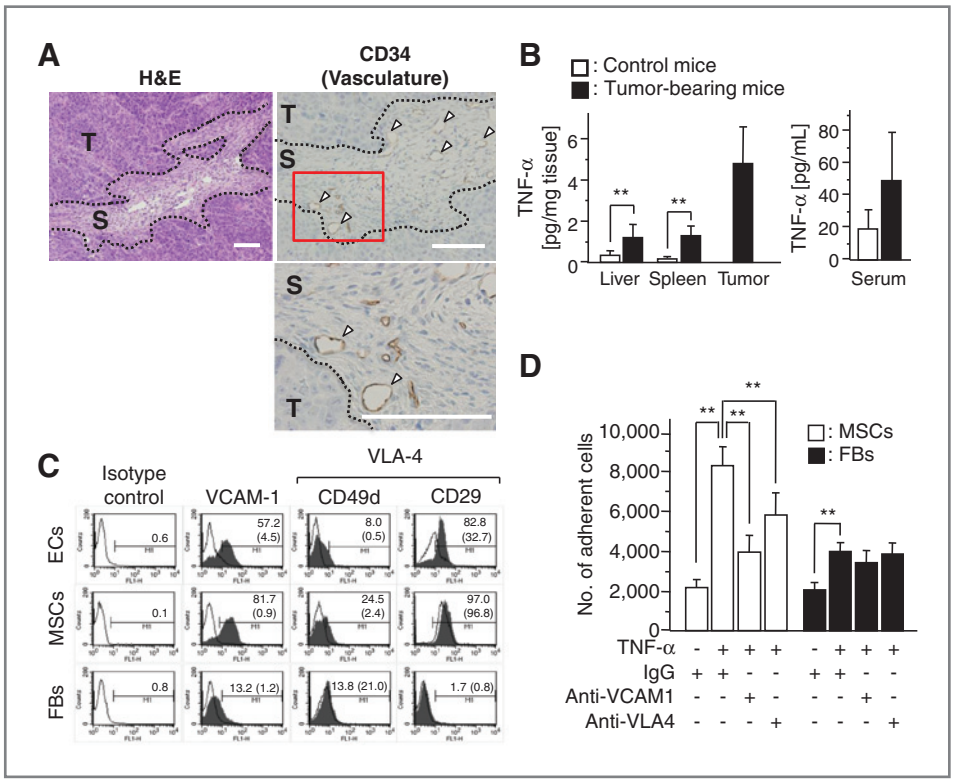

Figure 3. A, sections represent hematoxylin and eosin (H&E) staining (top left), the $CD34^+$ blood vessels/endothelial cells in tumor tissues (top right), the high-power field of view (bottom). Data shown are from 1 representative experiment of 3 carried out. Scale bar, 100 μm. S, stroma; T, tumor. B, specimens of tumor, liver, spleen, and blood were collected from control and tumor-bearing mice. TNF-α levels in tissue homogenates and serum were assayed by ELISA. *, $P < 0.05$; **, $P < 0.01$. C, MSCs, endothelial cells (EC), and fibroblasts were cultured with TNF-α (10 ng/mL) for 6 hours. Cells were labeled with FITC-conjugated antibodies and analyzed by flow cytometry (filled histogram). Rat isotype antibodies IgG1 and IgG2a served as respective controls (open histograms). Values represent the percentage of positive cells after TNF-α stimulation, and values in parentheses represent the percentage of positive cells without TNF-α stimulation. D, endothelial cells were cultured to confluence on fibronectin-coated 96-well plates. Then, MSCs or fibroblasts (1×10^4) were added to cultured endothelial cells. MSCs and endothelial cells were pretreated with the following substances: TNF-α (10 ng/mL), anti-VCAM-1, VLA-4 (10 μg/mL), or isotype control IgG. Values are mean ± SD. **, $P < 0.01$ ($n = 6$ per cell type).

that has been proposed for endothelial cell regulation of leukocyte infiltration in inflammatory tissues. Leukocyte-endothelial adhesion involves dynamic interactions between leukocytes and endothelial cells, and involves multiple steps. These steps must be precisely orchestrated to ensure a rapid response with minimal damage to healthy tissue (15). Interactions between leukocytes and the endothelium are mediated by several families of adhesion molecules, each of which participates in a different phase of the process. The surface expression and activation of these molecules during an inflammatory response is tightly controlled under normal conditions. Inflammatory cytokines including IL-1 and TNF-α involve induction of adhesion molecules. In our experimental settings, although other inflammatory cytokine levels including IL-1 and IL-6 were low (data not shown), significant production of TNF-α was observed. We do not clearly know the source of TNF-α in the tumor at this time, and that our *in vitro* data only suggest that the stroma is the primary source.

As we expected, TNF-α enabled MSCs to adhere to endothelial cells through induction of the expression of adhesion molecules, including VCAM-1 and VLA-4. It is generally considered that VCAM-1 on activated endothelium interacts with the VLA-4 on the leukocyte in the model of leukocyte–endothelial cell adhesion. At first, we speculated that VLA-4 on MSCs plays the same important role as leukocytes. Although both VCAM-1 and VLA-4 on endothelium were efficiently induced by TNF-α stimulation, TNF-α–induced expression of VCAM-1 on MSCs is much stronger than that of VLA-4. Furthermore, MSC–EC adhesion was more effectively inhibited by anti-VCAM-1 antibody as compared with the anti-VLA-4 antibody. On the basis of these results, although VLA-4 on MSC have also related to the MSC-EC adhesion, we thought that VCAM-1 on MSC has more important implications for this adhesion. Once MSCs circulate in the bloodstream, adhesion to endothelial cells is the first step in accumulation in tumors. TNF-α exerts its biologic functions through activating the NF-κB signaling pathway. NF-κB is a major cell survival signal that is antiapoptotic. MSC accumulation was significantly decreased through parthenolide inhibition of NF-κB activity. Although several studies have shown that mitogen-activated protein kinase (MAPK) phosphorylation by growth factors are involved in MSC migration (16, 17), parthenolide did not inhibit MAPK phosphorylation (data not shown). Therefore, at least parthenolide treatment did not affect in migration ability of

Published OnlineFirst October 12, 2012; DOI: 10.1158/0008-5472.CAN-12-0088

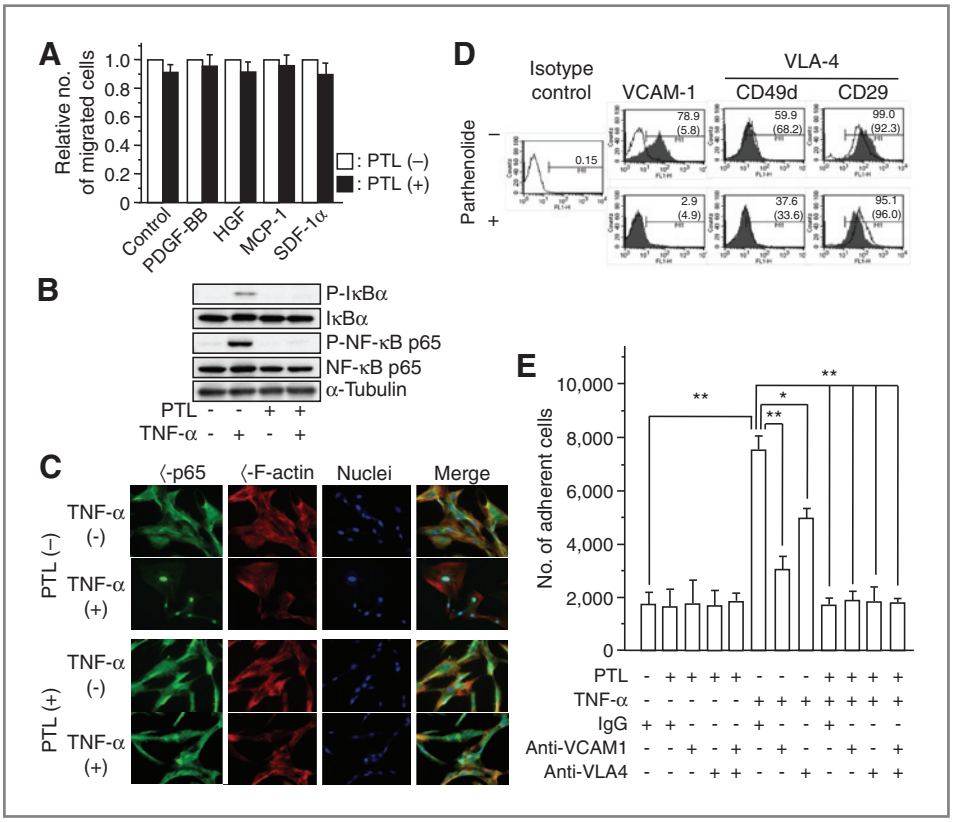

Figure 4. Effect of parthenolide (PTL) on MSC migration and adhesion. A, serum-starved and parthenolide-treated MSCs were added to the upper wells and serum-free medium supplemented with PDGF-BB (10 ng/mL), HGF (30 ng/mL), MCP-1 (100 ng/mL), or SDF-1α (150 ng/mL) was added to the lower wells. Treatment with medium alone (DMEM/F-12) was a negative control and treatment with 30% FBS was the positive control. Values are expressed by relative number of cells compared with respective controls (without pretreatment with parthenolide). B, to assess the inhibitory effect of parthenolide on NF-κB phosphorylation, parthenolide-treated MSCs were stimulated with recombinat TNF-α for 3 minutes, and cellular extracts were prepared for Western blotting. C, to monitor the inhibitory effect of parthenolide on NF-κB activation, immunofluorescent analysis of NF-κB p65 nuclear translocation was conducted as described in Materials and Methods with an Alexa Fluor 488–conjugated specific antibody (green). Actin filaments were labeled with Alexa Fluor 546–conjugated phalloidin (red); nuclei were stained with DRAQ-5 dye (blue). Objective magnification, ×40. D, effect of parthenolide treatment on TNF-α–induced expression of adhesion molecules was analyzed by flow cytometry. Parthenolide-treated MSCs were cultured with TNF-α (10 ng/mL) for 6 hours. Cells were labeled with FITC-conjugated antibodies and analyzed by flow cytometry (filled histogram). Rat isotype antibodies IgG1 and IgG2a served as respective controls (open histograms). Values represent the percentage of positive cells after TNF-α stimulation, and values in parentheses represent the percentage of positive cells without TNF-α stimulation. E, MSCs (1×10^4) were added to endothelial cells that had been cultured to confluence on fibronectin-coated 96-well plates. MSCs and endothelial cells were pretreated with the following substances: parthenolide (5 μmol/L), TNF-α (10 ng/mL), anti-VCAM-1, VLA-4 (10 μg/mL), or isotype control IgG. Values are expressed as mean ± SD ($n = 6$). *, $P < 0.05$ and **, $P < 0.01$.

MSCs toward growth factors from tumors in this experimental settings. Nevertheless, MSC accumulation was significantly decreased through parthenolide inhibition of NF-κB activity. We did not show histologic evidence in the experiments using parthenolide. However, we show that parthenolide does not inhibit luciferase activity *in vitro* (and thus does not seem to be toxic), and that therefore the effect observed *in vivo* should be an effect on recruitment. Although we focused on the function of TNF-α in this study, other inflammatory cytokines including IL-1β and IFN-γ also have ability to induce VCAM-1 expression in target cells (18), and may be involved in MSC accumulation.

TNF-α is a major inflammatory cytokine that plays important roles in diverse cellular events, such as cell survival, proliferation, differentiation, and death. Numerous reports have shown that TNF-α levels in serum are increased in patients with cancer (19, 20), and TNF-α is also related closely to the tumor progression including metastasis. For example, TNF-α intensely induces IL-6 and MCP-1 from cancer-associated fibroblasts and normal fibroblastic cells and has indirect influences on generation of prometastatic microenvironment (21). Furthermore, TNF-α is also released in cardiac infarction, during acute coronary syndromes, and in chronic heart failure; MSCs also accumulate at the site of cardiac infarction (22, 23). These results indicated that proinflammatory cytokines promote homing of stem cells in the heart and that these cytokines have a positive effect on cardiac regeneration. Therefore, activation with TNF-α is one of the critically important steps for MSC accumulation. Moreover, MSC-based tissue-targeted strategies may be adapted for various inflammatory diseases.

In MSC-based cancer-targeted gene therapies, it is thought that therapeutic efficacy is directly linked with accumulation efficiency of MSCs at tumor sites. Our results suggested that combination use of NF-κB inhibitors, including bortezomib, or TNF-α blocking agents, such as infliximab, reduces the

Published OnlineFirst October 12, 2012; DOI: 10.1158/0008-5472.CAN-12-0088

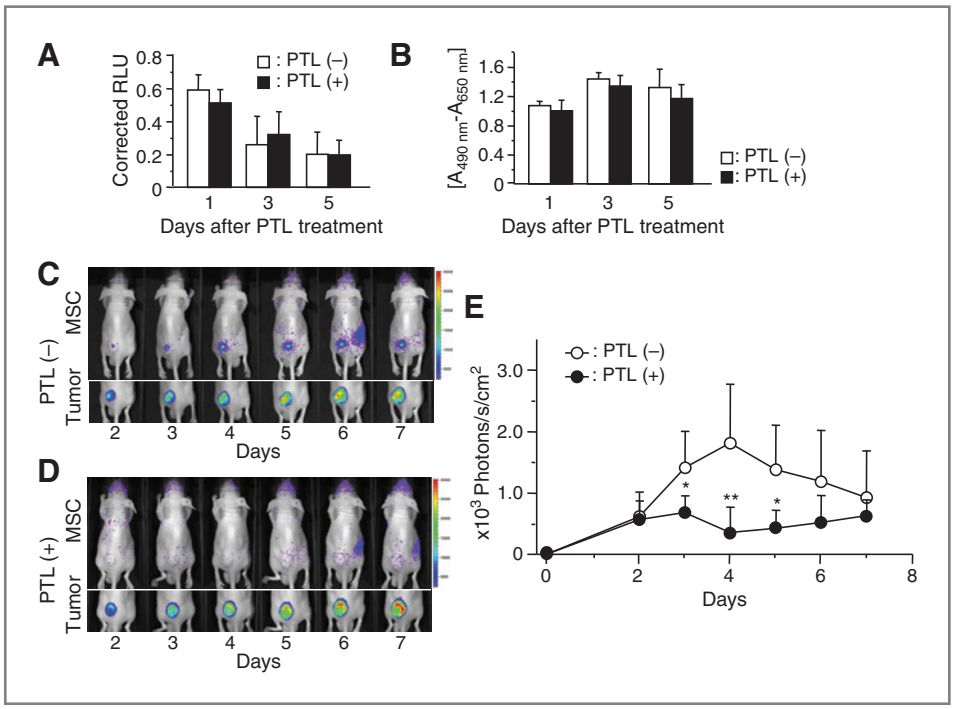

Figure 5. *In vivo* imaging of NF-κB–suppressed MSC accumulation at tumor sites. A, luciferase-expressing MSCs were cultured with parthenolide for 6 hours and luciferase assays were periodically conducted. Values are expressed as mean ± SD ($n = 4$ each). RLU, relative light unit. B, cell viability of parthenolide (PTL)-treated luciferase-expressing MSCs was also examined by XTT assays. Values are expressed as mean ± SD ($n = 4$ each). C, luciferase-expressing MSCs without parthenolide treatment were injected into tumor-bearing mice through the left ventricular cavity and IVIS imaging was periodically conducted. Each data shown are from 1 representative experiment of 8 carried out. D, luciferase-expressing MSCs with parthenolide treatment were injected into tumor-bearing mice and IVIS imaging was periodically conducted. Imaging was conducted as described earlier. Each data shown are from 1 representative experiment of 8 carried out. E, bioluminescent intensity at tumor sites was quantified using analysis software. The data are expressed as mean ± SD ($n = 8$ each). *, $P < 0.05$; **, $P < 0.01$ compared with a group of parthenolide (–) at the same time.

therapeutic efficacy of gene-modified MSCs due to inhibition of the accumulation steps. In contrast, tumor-specific TNF-α–inducing agents would be useful in enhancing therapeutic efficacy, thus further research is required in identifying such agents to more effective therapeutic strategies.

In conclusion, the present study shows that NF-κB activation through TNF-α stimulation and VCAM-1/VLA-4–mediated MSC-EC adhesion may be an important element in MSC accumulation. Although MSCs are useful as cellular vehicles for cancer-targeted gene therapy, past studies have shown that increased MSC accumulation is needed to enhance therapeutic efficacy. Thus, methodology for the enhancement of MSC accumulation should be developed and our findings suggest a solution.

Disclosure of Potential Conflicts of Interest

No potential conflicts of interest were disclosed.

Authors' Contributions

Conception and design: R. Uchibori, H. Mizukami, K. Ozawa
Development of methodology: M. Urabe
Acquisition of data (provided animals, acquired and managed patients, provided facilities, etc.): R. Uchibori
Analysis and interpretation of data (e.g., statistical analysis, biostatistics, computational analysis): R. Uchibori, H. Mizukami, A. Kume
Writing, review, and/or revision of the manuscript: R. Uchibori, M. Urabe, A. Kume
Administrative, technical, or material support (i.e., reporting or organizing data, constructing databases): T. Tsukahara, H. Mizuguchi, Y. Saga, K. Ozawa
Study supervision: M. Urabe, A. Kume, K. Ozawa

Acknowledgments

The authors thank Miyoko Mitsu for her encouragement and technical support.

Grant Support

This work was supported by Grant-in-Aid for Scientific Research (KAKENHI) from the Ministry of Education, Culture, Sports, Science and Technology (21390296 to K. Ozawa), and The Research Award to Jichi Medical School Graduate Student (to R. Uchibori).

The costs of publication of this article were defrayed in part by the payment of page charges. This article must therefore be hereby marked *advertisement* in accordance with 18 U.S.C. Section 1734 solely to indicate this fact.

Received January 13, 2012; revised August 30, 2012; accepted September 11, 2012; published OnlineFirst October 12, 2012.

References

1. Studeny M, Marini FC, Champlin RE, Zompetta C, Fidler IJ, Andreeff M. Bone marrow-derived mesenchymal stem cells as vehicles for interferon-beta delivery into tumors. Cancer Res 2002;62:3603–8.

Published OnlineFirst October 12, 2012; DOI: 10.1158/0008-5472.CAN-12-0088

2. Studeny M, Marini FC, Dembinski JL, Zompetta C, Cabreira-Hansen M, Bekele BN, et al. Mesenchymal stem cells: potential precursors for tumor stroma and targeted-delivery vehicles for anticancer agents. J Natl Cancer Inst 2004;96:1593–603.
3. Nakamizo A, Marini F, Amano T, Khan A, Studeny M, Gumin J, et al. Human bone marrow-derived mesenchymal stem cells in the treatment of gliomas. Cancer Res 2005;65:3307–18.
4. Chen X, Lin X, Zhao J, Shi W, Zhang H, Wang Y, et al. A tumor-selective biotherapy with prolonged impact on established metastases based on cytokine gene-engineered MSCs. Mol Ther 2008;16:749–56.
5. Xin H, Kanehira M, Mizuguchi H, Hayakawa T, Kikuchi T, Nukiwa T, et al. Targeted delivery of CX3CL1 to multiple lung tumors by mesenchymal stem cells. Stem Cells 2007;25:1618–26.
6. Uchibori R, Okada T, Ito T, Urabe M, Mizukami H, Kume A, et al. Retroviral vector-producing mesenchymal stem cells for targeted suicide cancer gene therapy. J Gene Med 2009;11:373–81.
7. Dwyer RM, Potter-Beirne SM, Harrington KA, Lowery AJ, Hennessy E, Murphy JM, et al. Monocyte chemotactic protein-1 secreted by primary breast tumors stimulates migration of mesenchymal stem cells. Clin Cancer Res 2007;13:5020–7.
8. Mizuguchi H, Kay MA. Efficient construction of a recombinant adenovirus vector by an improved *in vitro* ligation method. Hum Gene Ther 1998;9:2577–83.
9. Mizuguchi H, Kay MA. A simple method for constructing E1- and E1/E4-deleted recombinant adenoviral vectors. Hum Gene Ther 1999;10:2013–7.
10. Koizumi N, Mizuguchi H, Utoguchi N, Watanabe Y, Hayakawa T. Generation of fiber-modified adenovirus vectors containing heterologous peptides in both the HI loop and C terminus of the fiber knob. J Gene Med 2003;5:267–76.
11. Mittereder N, March KL, Trapnell BC. Evaluation of the concentration and bioactivity of adenovirus vectors for gene therapy. J Virol 1996;70:7498–509.
12. Coussens LM, Werb Z. Inflammation and cancer. Nature 2002;420:860–7.
13. Honczarenko M, Le Y, Swierkowski M, Ghiran I, Glodek AM, Silberstein LE. Human bone marrow stromal cells express a distinct set of biologically functional chemokine receptors. Stem Cells 2006;24:1030–41.
14. Rüster B, Göttig S, Ludwig RJ, Bistrian R, Müller S, Seifried E, et al. Mesenchymal stem cells display coordinated rolling and adhesion behavior on endothelial cells. Blood 2006;108:3938–44.
15. Butcher EC. Leukocyte-endothelial cell recognition: three (or more) steps to specificity and diversity. Cell 1991;67:1033–6.
16. Coffelt SB, Marini FC, Watson K, Zwezdaryk KJ, Dembinski JL, LaMarcad HL, et al. The pro-inflammatory peptide LL-37 promotes ovarian tumor progression through recruitment of multipotent mesenchymal stromal cells. Proc Natl Acad Sci U S A 2009;106:3806–11.
17. Zhang A, Wang Y, Ye Z, Xie H, Zhou L, Zheng S. Mechanism of TNF-α-induced migration and hepatocyte growth factor production in human mesenchymal stem cells. J Cell Biochem 2010;111:469–75.
18. Hosokawa Y, Hosokawa I, Ozaki K, Nakae H, Matsuo T. Cytokines differentially regulate ICAM-1 and VCAM-1 expression on human gingival fibroblasts. Clin Exp Immunol 2006;144:494–502.
19. Ferrajoli A, Keating MJ, Manshouri T, Giles FJ, Dey A, Estrov Z, et al. The clinical significance of tumor necrosis factor-alpha plasma level in patients having chronic lymphocytic leukemia. Blood 2002;100:1215–9.
20. Ahmed MI, Salahy EE, Fayed ST, El-Hefnawy NG, Khalifa A. Human papillomavirus infection among Egyptian females with cervical carcinoma: relationship to spontaneous apoptosis and TNF-alpha. Clin Biochem 2001;34:491–8.
21. Mueller L, von Seggern L, Schumacher J, Goumas F, Wilms C, Braun F, et al. TNF-alpha similarly induces IL-6 and MCP-1 in fibroblasts from colorectal liver metastases and normal liver fibroblasts. Biochem Biophys Res Commun 2010;397:586–91.
22. Shake JG, Gruber PJ, Baumgartner WA, Senechal G, Meyers J, Redmond JM, et al. Mesenchymal stem cell implantation in a swine myocardial infarct model: engraftment and functional effects. Ann Thorac Surg 2002;73:1919–25.
23. Pittenger MF, Martin BJ. Mesenchymal stem cells and their potential as cardiac therapeutics. Circ Res 2004;95:9–20.

Cancer Research
The Journal of Cancer Research (1916–1930) | The American Journal of Cancer (1931–1940)

AACR American Association for Cancer Research

NF-κB Activity Regulates Mesenchymal Stem Cell Accumulation at Tumor Sites

Ryosuke Uchibori, Tomonori Tsukahara, Hiroyuki Mizuguchi, et al.

Cancer Res Published OnlineFirst October 12, 2012.